Raman Spectra of the Solid-Solution between $Rb_2La_2Ti_3O_{10}$ and $RbCa_2Nb_3O_{10}$

Hee Jin Kim, Song-Ho Byeon,[*] and Hoseop Yun[†]

College of Environment and Applied Chemistry, Kyung Hee University, Kyung Ki 449-701, Korea
[†]Department of Chemistry, Ajou University, Kyung Ki 442-749, Korea
Received October 9, 2000

A site preference of niobium atom in $Rb_{2-x}La_2Ti_{3-x}Nb_xO_{10}$ ($0.0 \leq x \leq 1.0$) and $RbLa_{2-x}Ca_xTi_{2-x}Nb_{1+x}O_{10}$ ($0.0 \leq x \leq 2.0$), which are the solid-solutions between $Rb_2La_2Ti_3O_{10}$ and $RbCa_2Nb_3O_{10}$, has been investigated by Raman spectroscopy. The Raman spectra of $Rb_{2-x}La_2Ti_{3-x}Nb_xO_{10}$ ($0.0 \leq x \leq 1.0$) gave an evidence that niobium atoms substituted for titanium atoms preferably occupy the highly distorted outer octahedral sites rather than the central ones in triple-octahedral perovskite layers. In contrast, the Raman spectra of $RbLa_{2-x}Ca_xTi_{2-x}Nb_{1+x}O_{10}$ ($0.0 \leq x \leq 2.0$) showed no clear information for the cationic arrangement in perovskite slabs. This difference indicated that a site preference of niobium atoms is observed only when the linear Rb-O-Ti linkage can be replaced by much stronger terminal Nb-O bond with double bond character. From comparison with the Raman spectroscopic behavior of $CsLa_{2-x}A'_xTi_{2-x}Nb_{1+x}O_{10}$ (A' = Ca and Ba; $0.0 \leq x \leq 2.0$), it is also proposed that a local difference in arrangement of interlayer atoms causes a significantly different solid acidity and photocatalytic activity of the layered perovskite oxides, despite their crystallographically similar structures.

Kywords : Layered structure, Oxides, Raman spectra, Site preference.

Introduction

The oxides containing Ti and Nb have potential applications in the photocatalytic decomposition of H_2O. Some examples of them could be referred to $SrTiO_3$, $K_4Nb_6O_{17}$, $Na_2Ti_6O_{13}$, $BaTi_4O_9$, $K_2Ti_4O_9$, $K_2La_2Ti_3O_{10}$, $Na_2Ti_3O_7$, $La_2Ti_2O_7$, and $A_2Nb_2O_7$ (A=Ca, Sr).[1-8] Many of such examples have a layered structure. In particular, a typical layered perovskite $A_{2-x}La_2Ti_{3-x}Nb_xO_{10}$ (A=K, Rb, Cs) solid-solution showed high photocatalytic activity for the water splitting[9,10] The remarkable shape selectivity and dependence of the catalytic activity on x value suggested an important role of the interlayer space.

An arrangement of niobium and titanium atoms in the octahedral perovskite slabs of $ACa_{2-x}La_xNb_{3-x}Ti_xO_{10}$ (A=alkali-metals) were also investigated by two research groups. A significant change in the solid acidity of their protonated phases, $HCa_{2-x}La_xNb_{3-x}Ti_xO_{10}$, induced a following suggestion: The corner shared triple-octahedra are ordered in the sequence of NbO_6-TiO_6-NbO_6-along the c axis in $ACaLaNb_2TiO_{10}$ (x=1), but the ordering of niobium and titanium atoms is reversed in $ALa_2NbTi_2O_{10}$ (x=2), the niobium atoms occupying central octahedra.[11] In contrast, the structural analyses of the same series gave a completely different conclusion such that the cationic arrangements are in the sequence of -$(Ti_{0.15}Nb_{0.85})O_6$-$(Ti_{0.7}Nb_{0.3})O_6$-$(Ti_{0.15}Nb_{0.85})O_6$- and -$(Ti_{0.5}Nb_{0.5})O_6$-TiO_6-$(Ti_{0.5}Nb_{0.5})O_6$- along the c axis in $ACaLaNb_2TiO_{10}$ and $ALa_2NbTi_2O_{10}$, respectively.[12]

The Raman spectroscopic approach may give a supporting evidence for a site preference of niobium atoms in the octahedral slabs of layered perovskite structure. Recent study has been focused on the relationship between interlayer structure and Raman spectra of ion-exchangeable layered perovskites.[13] An interesting feature observed in such works

was that the correlation between triple-octahedral layer and interlayer structure is significantly different depending on their connection mode. An existence or absence of the linear linkage between them could be confirmed by the characteristic band around 850-950 cm^{-1} without knowledge of the exact crystal structure.

In this work, the Raman spectra of $Rb_{2-x}La_2Ti_{3-x}Nb_xO_{10}$ ($0.0 \leq x \leq 1.0$) and $ALa_{2-x}A'_xTi_{2-x}Nb_{1+x}O_{10}$ ($0.0 \leq x \leq 2.0$; A = Rb, Cs; A'=Ca, Ba) solid-solutions were examined to investigate a cationic arrangement and bonding nature in octahedral layer and interlayer space. The spectral interpretation was based on the previous reference Raman spectra of $Rb_2La_2Ti_3O_{10}$ and $ACa_2Nb_3O_{10}$ (A=Rb and Cs), which are the end members of such solid-solutions. Interestingly, a good evidence was given for a site preference of niobium atoms in triple-octahedral perovskite slabs as well as a significant local change of interlayer structure in the solid-solution range.

Experimental Section

$Rb_{2-x}La_2Ti_{3-x}Nb_xO_{10}$ ($0.0 \leq x \leq 1.0$) and $ALa_{2-x}A'_xTi_{2-x}Nb_{1+x}O_{10}$ ($0.0 \leq x \leq 2.0$; A=Rb, Cs; A'=Ca, Ba) solid-solutions were prepared by heating appropriate mixture of A_2CO_3, La_2O_3, $A'CO_3$, Nb_2O_5, and TiO_2 in air at 1000-1150 °C for 2 days with two intermittent grindings.[3-7] An excess (~20 mol %) of A_2CO_3 was added to compensate for the loss of volatile alkali-metal components. After the reaction, the products were washed with distilled water and dried at 120 °C.

A stoichiometric composition was confirmed by the elemental analysis of alkali-metal using the inductively coupled plasma (ICP) and the energy-dispersive X-ray emission (EDX) techniques. The formation of single phase was con-

firmed by the powder X-ray diffraction (XRD). All the patterns of prepared oxides in this work were indexed on the basis of tetragonal or orthorhombic cell and in well agreement with the literature data.[11,14-17]

Raman spectra were obtained with a Bruker RFS 100/S FT-Raman spectrometer coupled to the high sensitivity Raman detector (Model D 418-S), which was cooled down to liquid nitrogen temperature. Powdered samples packed into small aluminum cups were excited by the 1064-nm line of the Nd:YAG laser with 10 mW of power. The laser beam was focused on the sample and the scattered light was collimated into the spectrometer by 180° angle configuration. Raman spectra were collected at room temperature. The overall spectral resolution of the spectra was determined to be about 2 cm^{-1}.

Results and Discussion

The structures of end members, $Rb_2La_2Ti_3O_{10}$ and $RbCa_2Nb_3O_{10}$, for solid-solution are schematically compared in Figure 1. In the structure of $Rb_2La_2Ti_3O_{10}$, the perovskite slab is composed of corner shared triple-TiO_6 octahedra and the adjacent slabs have the staggered conformation leading to the c axis doubling. The Rb atoms occupy all of 9-coordinate sites in the interlayer space as shown in Figure 1a. A displacement of titanium atom from the center of its octahedron toward rubidium atom layers gives highly distorted outer octahedral layers and slightly distorted central one.[13,18] The corner shared TiO_6 octahedra are relatively rotated

($\sim 12.5^{\circ}$) and tilted about the c axis. Although overall feature of triple-NbO_6 octahedral layer is also true for $RbCa_2Nb_3O_{10}$, on the contrary, the interlayer rubidium atoms occupy distorted cubic sites which are given by the eclipsed conformation of adjacent perovskite slabs (Figure 1b). Thus, it should be noted that the structures of end members have an important difference in bonding nature of rubidium atom. There is a practically linear Rb-O-Ti linkage parallel to the c axis in $Rb_2La_2Ti_3O_{10}$. Due to this structural feature, the competing Ti-O bond vibration was sensitively changed depending on the interlayer structure. In contrast, no linear Rb-O-Nb connection is there in the structure of $RbCa_2Nb_3O_{10}$. Accordingly, the interlayer structure did not greatly affect the Nb-O terminal bond with double bond character.

Based on the previous report,[13] the local structural difference between two end members is reflected quite well in their Raman spectra when the interlayer atoms are changed. Figure 2 shows the Raman spectra of $A_2La_2Ti_3O_{10}$ (A=Na, K, and Rb). The bands around 900-860 cm^{-1} and around 580-540 and 520-510 cm^{-1} are assigned to the symmetric stretching mode and the asymmetric modes of highly distorted outer TiO_6 octahedra, respectively. The band around 700-670 cm^{-1} is related to the slightly distorted central TiO_6 octahedra. The bands below 400 cm^{-1} are assigned to external modes located in the alkali-metal layer. A considerable shift of the band at 902 cm^{-1} ($Na_2La_2Ti_3O_{10}$), which is assigned to the stretching mode of short Ti-O bond along the c axis, to 875 ($K_2La_2Ti_3O_{10}$) and 867 cm^{-1} ($Rb_2La_2Ti_3O_{10}$) reflects an existence of linear A-O-Ti linkage. In contrast, no significant shift of this band is observed in spite of a large
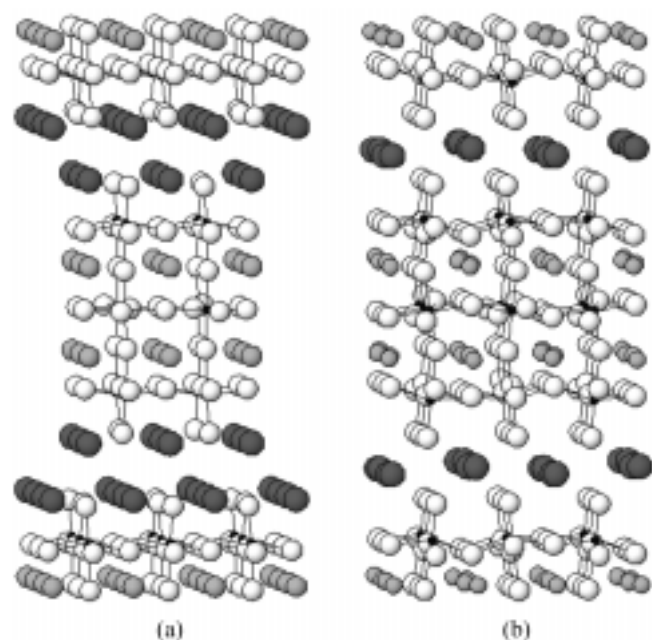

Figure 1. Schematic illustrations of the structure for (a) Rb₂La₂-Ti₃O₁₀ and (b) RbCa₂Nb₃O₁₀ perpendicular to the c direction of the tetragonal or orthorhombic unit cell. The triple-octahedral unit is composed of the highly distorted outer octahedra and the slightly distorted central octahedra. Small shaded spheres, large shaded spheres, black spheres, and white spheres are La or Ca, Rb, Ti or Nb, and O atoms, respectively.
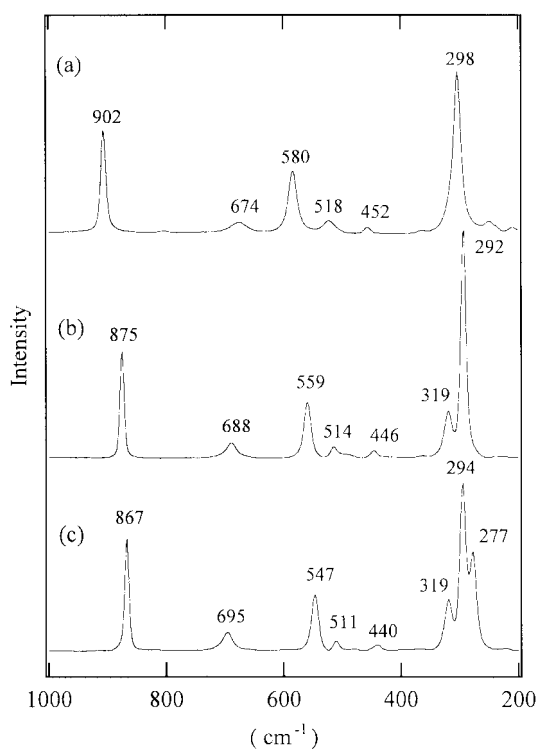

Figure 2. The Raman spectra of (a) Na₂La₂Ti₃O₁₀, (b) K₂La₂Ti₃-O₁₀, and (c) Rb₂La₂Ti₃O₁₀.
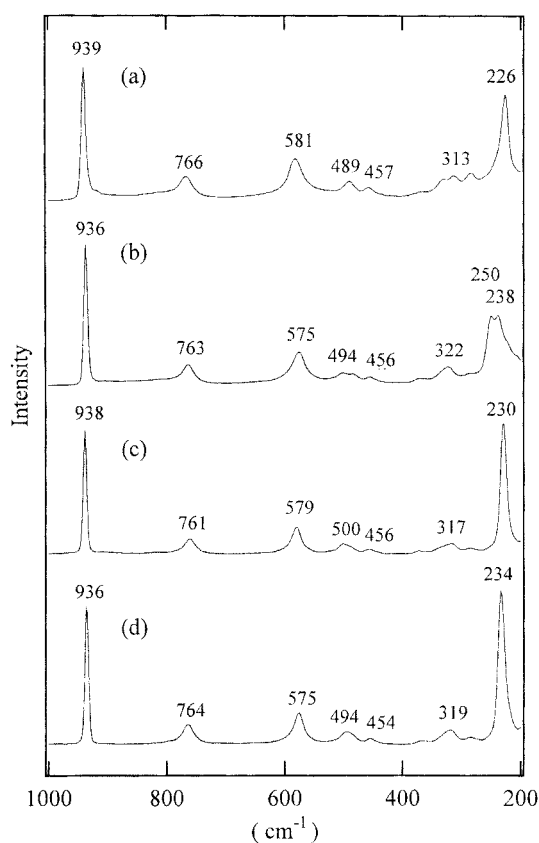
Figure 3. The Raman spectra of (a) $NaCa_2Nb_3O_{10}$, (b) $KCa_2Nb_3O_{10}$, (c) $RbCa_2Nb_3O_{10}$, and (d) $CsCa_2Nb_3O_{10}$.

Figure 4. The Raman spectra of $Rb_{2-x}La_2Ti_{3-x}Nb_xO_{10}$ with (a) $x=$ 0.0, (b) $x=0.25$, (c) $x=0.5$, (d) $x=0.75$, and (e) $x=1.0$.

lattice expansion if such a linear connection is absent.

Figure 3 shows the Raman spectra of $ACa_2Nb_3O_{10}$ (A= Na, K, Rb, and Cs) whose structure contains no linear A-O-Nb linkage. A sharp strong band around 936 cm^{-1} is assigned to the vibrational mode of the Nb-O terminal bond of highly distorted NbO_6 octahedra. The bands around 580 and 490 cm^{-1} are also attributed to the highly distorted NbO_6 octahedra. The band around 760 cm^{-1} is due to the slightly distorted central NbO_6 octahedra. Essentially constant Raman bands in the region 400-1000 cm^{-1} regardless of the change of alkali-metal layers are associated with the absence of linear A-O-Nb connection in the structure of $ACa_2Nb_3O_{10}$.

In attempts to provide an information for a cationic arrangement and bonding nature in perovskite layer and interlayer space, the Raman spectra of $Rb_{2-x}La_2Ti_{3-x}Nb_xO_{10}$ ($0.0 \leq x \leq 1.0$) were examined. This solid-solution corresponds to a bridging system of $Rb_2La_2Ti_3O_{10}$ and $RbLa_2Ti_2NbO_{10}$. Their Raman spectra are compared as a function of x value in Figure 4. A remarkable shift and broadening of the band at 867 cm^{-1} is induced with increasing x. Its relative intensity also largely decreases and this band ultimately disappears in the spectrum of $RbLa_2Ti_2NbO_{10}$ ($x=1.0$). A new weak band at 957 cm^{-1} appears when $x=0.25$ and becomes more intense with increasing x. This dramatic change is explained as follows: The niobium atoms substituted for the titanium ones may preferably occupy the highly distorted outer octahedral layer of triple-perovskite slab to form the terminal Nb-O
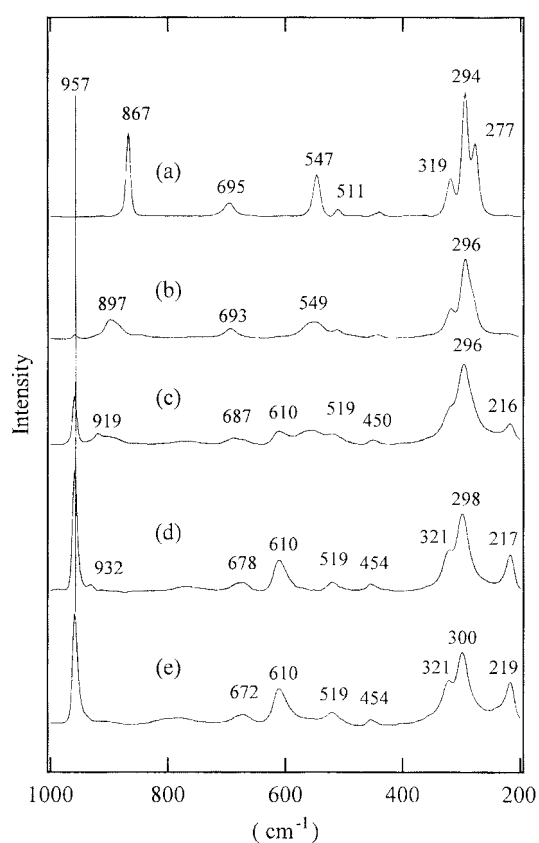
bond, giving rise to the band at 957 cm^{-1}. Due to the induced vacancies in the interlayer spaces, the Rb-O-Ti bond deviates from a linear connection with increasing x. A strengthening of Ti-O bond then leads the band at 867 cm^{-1} to shift toward higher frequency. Such an assumption is supported by the fact that the intensity of the band at 957 cm^{-1} is proportional to the amount of replaced niobium atoms but no shift of this band is observed regardless of x. The site preference of niobium atom is also consistent with a considerable broadening and weakening of the band at 547 cm^{-1} which is attributed to the highly distorted outer TiO_6 octahedra. A disappearance of this band is accompanied by an increased intensity of the band at 610 cm^{-1} which appears from $x=0.5$, indicating that this new band is associated with the highly distorted outer (Ti, Nb)O_6 octahedra. Although its relative intensity is not significant, a weak band appeared at ~760 cm^{-1} suggests a formation of small amount of central NbO_6 octahedra. No observation of the bands at 867 and 547 cm^{-1} when $x=1$ ($RbLa_2Ti_2NbO_{10}$) therefore reflects an absence of linear Rb-O-Ti connection despite that a number of outer octahedral sites are still occupied by titanium atoms. The central TiO_6-related mode (695 cm^{-1}-band) shows only a small and gradual shift toward lower frequency. This indicates that the increased occupancy of niobium atoms for the outer octahedral sites decreases the covalent character of the central TiO_6 octahedra. This explanation is relatively in agreement with previous structural data having proposed an
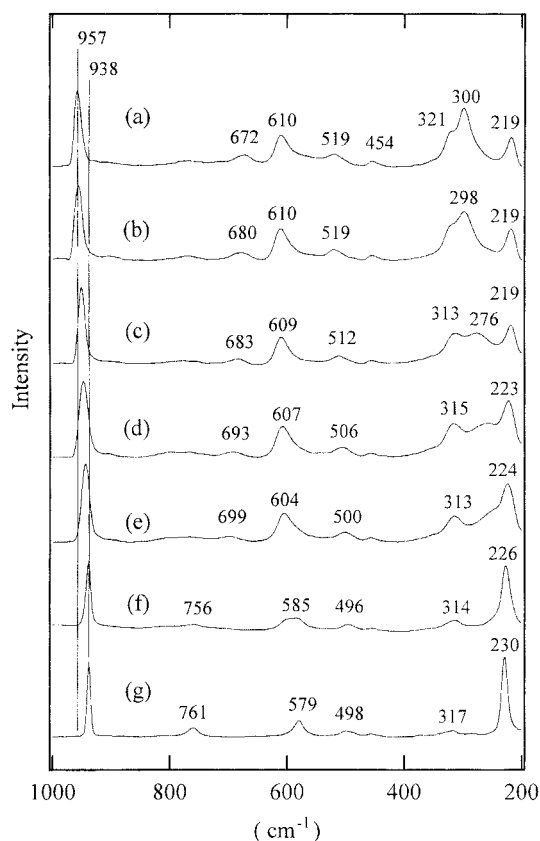
Figure 5. The Raman spectra of $RbLa_{2-x}Ca_xTi_{2-x}Nb_{1+x}O_{10}$ with (a) $x=0.0$, (b) $x=0.5$, (c) $x=1.0$, (d) $x=1.2$, (e) $x=1.5$, (f) $x=1.8$, and (g) $x=2.0$.

Figure 6. The Raman spectra of $CsLa_{2-x}Ca_xTi_{2-x}Nb_{1+x}O_{10}$ with (a) $x=0.0$, (b) $x=0.5$, (c) $x=1.0$, (d) $x=1.2$, (e) $x=1.5$, (f) $x=1.8$, and (g) $x=2.0$.

octahedral arrangement -$(Ti_{0.5}Nb_{0.5})O_6$-TiO_6-$(Ti_{0.5}Nb_{0.5})O_6$- along the *c* axis for $RbLa_2Ti_2NbO_{10}$.[12] As evidenced by an observation of weak band at ~760 cm⁻¹, however, an existence of central NbO_6 octahedra should not be completely ignored for this phase.

Further replacement of titanium atoms by niobium ones was extended to a $RbLa_{2-x}Ca_xTi_{2-x}Nb_{1+x}O_{10}$ $(0.0 \leq x \leq 2.0)$ series. This system corresponds to a solid-solution between $RbLa_2Ti_2NbO_{10}$ and $RbCa_2Nb_3O_{10}$. The preference of niobium atoms for the outer octahedral sites was however not evident for this system in which there is no linear Rb⁻O⁻Ti bond. As shown in Figure 5, the band at 957 cm⁻¹ related to the terminal Nb-O bond gradually narrows and shifts toward 938 cm⁻¹ with increasing *x*. Similar shift toward lower frequency is observed for the band at 610 cm⁻¹. On the contrary, a gradual weakening and shift toward higher frequency of the central octahedra-related band around 672 cm⁻¹ is induced as *x* increases. Hence, it is most likely that the central TiO_6 octahedra are replaced by more covalent NbO_6 ones in proportion to *x*. This indicates that the relative occupancy of niobium atom becomes gradually higher for the central octahedral sites rather than for the outer octahedral ones with increasing *x*. The enhanced average covalent character of the central (Ti, Nb)O_6 octahedra reduces in turn the covalent character of highly distorted outer octahedra, resulting in a gradual shift of the bands at 957 and 610 cm⁻¹ toward lower frequency.
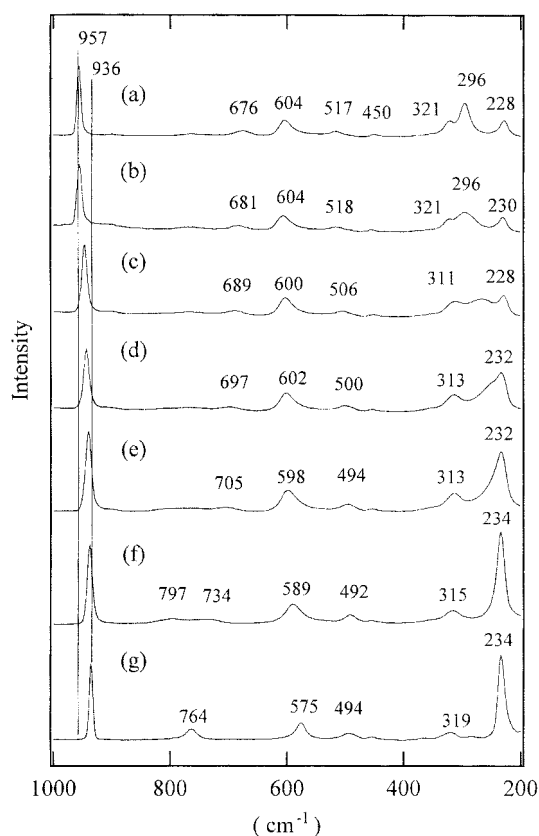
The Raman spectral characteristics of $CsLa_{2-x}Ca_xTi_{2-x}Nb_{1+x}$-$O_{10}$ shown in Figure 6 are quite similar to those of $RbLa_{2-x}$-$Ca_xTi_{2-x}Nb_{1+x}O_{10}$ solid-solution, indicating that they are iso-structural. All of Raman behaviors are also true for $CsLa_{2-x}$-$Ba_xTi_{2-x}Nb_{1+x}O_{10}$ system which has much larger lattice volume (Figure 7). In particular, the bands attributed to the central (Ti, Nb)O_6 octahedra (699 and 705 cm⁻¹ in Figures 5(c) and 6(c), respectively) are observed until $x=1.5$ ($ALa_{0.5}$-$Ca_{1.5}Ti_{0.5}Nb_{2.5}O_{10}$). Thus, both the central and outer TiO_6 octahedra are likely to exist over all solid-solution range. This would be in agreement with a proposed octahedral arrangement -$(Ti_{0.15}Nb_{0.85})O_6$-$(Ti_{0.7}Nb_{0.3})O_6$-$(Ti_{0.15}Nb_{0.85})O_6$- along the *c* axis for $CsLaCaTiNb_2O_{10}$ ($x=1$).[12]

As a consequence, it can be proposed that a site preference is observed when the linear A-O-Ti linkage can be replaced by much stronger terminal Nb-O bond with double bond character and therefrom a considerable decrease of lattice energy can be achieved. One more evidence supporting such a conclusion could be referred to the cationic arrangement in triple-octahedral layer of $Li_2La_{1.78}(Nb_{0.66}Ti_{2.34})O_{10}$.[19] The structure of this oxide can be derived from $Li_2La_2Ti_3O_{10}$ which is isostructural with $A_2La_2Ti_3O_{10}$ (A=K and Rb).[15] When titanium atoms are partially replaced by niobium atoms, most of them occupy the outer octahedral sites (in the sequence of -$(Ti_{0.69}Nb_{0.31})O_6$-$(Ti_{0.96}Nb_{0.04})O_6$-$(Ti_{0.69}Nb_{0.31})O_6$-). The lithium atoms occupy the distorted tetrahedral sites in the inter-layer space, giving terminal Nb-O bonds.

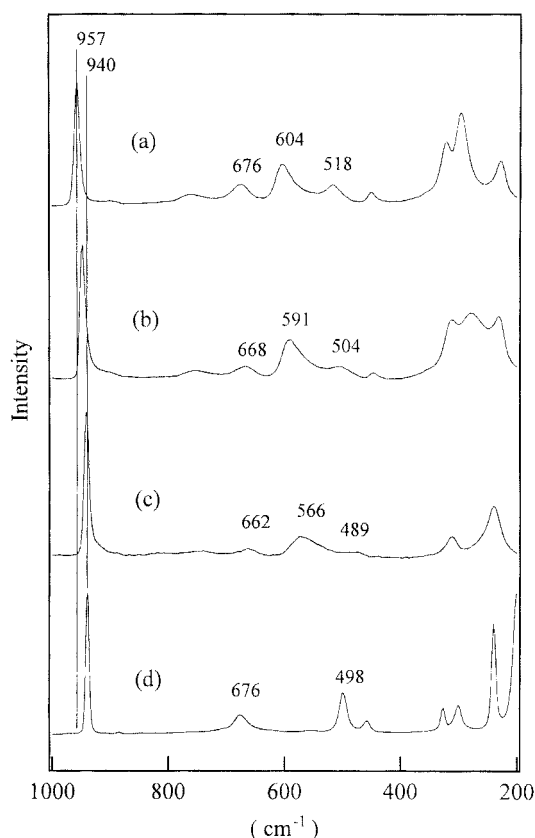**Figure 7**. The Raman spectra of $CsLa_{2-x}Ba_xTi_{2-x}Nb_{1+x}O_{10}$ with (a) x=0.0, (b) x=0.5, (c) x=1.0, and (d) x=2.0.

However, one of the important aspects to be pointed out is the considerable change of the bands at 200-400 cm^{-1} which are related to the interlayer structure. Although the coordination environment for cesium or rubidium atoms was regarded as the same in the structural analysis of $ALa_2Ti_2NbO_{10}$, $ALaCaTiNb_2O_{10}$, and $ACa_2Nb_3O_{10}$,[12] present Raman spectra clearly shows that rubidium or cesium layers are continuously rearranged until all of titanium atoms are replaced by niobium ones. Thus, the arrangement of interlayer atoms is closely dependent of the NbO_6/TiO_6 ratio in the outer octahedral layer of triple-perovskite slab. A local difference in the interlayer structure would be accordingly responsible for the quite different photocatalytic activities[9] of $A_2La_2Ti_3O_{10}$, $A_{1.5}La_2Ti_{2.5}Nb_{0.5}O_{10}$, and $ALa_2Ti_2NbO_{10}$ (A=K, Rb, Cs) and solid acidity[11] of $H_2La_2Ti_3O_{10}$, $HLa_2Ti_2NbO_{10}$, and $HCa_2Nb_3O_{10}$.

In conclusion, although they have crystallographically similar structure, the layered perovskite oxides can give a significantly different interlayer chemistry depending on the local structure of interlayer space. In this point of view, the Raman spectroscopy could be an efficient tool for the confirmation of local structural change during a chemical reaction in the interlayer space of layered perovskite.

References

1. Domen, K.; Naito, S.; Ohnish, T.; Tamaru, K. *Chem. Phys. Lett.* **1982**, *92*, 433.
2. Kudo, A.; Tanaka, A.; Domen, K.; Maruya, K.; Aika, K.; Ohnish, T. *J. Catal.* **1988**, *111*, 67.
3. Inoue, Y.; Kubokawa, T.; Sato, K. *J. Chem. Soc. Chem. Commun.* **1990**, 1298.
4. Inoue, Y.; Niiyama, T.; Asai, Y.; Sato, Y. *J. Chem. Soc. Chem. Commun.* **1992**, 579.
5. Uchida, S.; Yamamoto, Y.; Fujishiro, Y.; Watanabe, A.; Itoh, O.; Sato, T. *J. Chem. Soc. Dalton Trans.* **1997**, *93*, 3229.
6. Ikeda, S.; Hara, M.; Kondo, J. N.; Domen, K.; Takahashi, H.; Okubo, T.; Kakihana, M. *Chem. Mater.* **1998**, *10*, 72.
7. Ogura, S.; Kohno, M.; Sato, K.; Inoue, Y. *J. Mater. Chem.* **1998**, *8*, 2335.
8. Kim, H.; Hwang, D.; Kim, J.; Kim, Y.; Lee, J. *Chem. Commun.* **1999**, 1077.
9. Takata, T.; Furumi, Y.; Shinohara, K.; Tanaka, A.; Hara, M.; Kondo, J.; Domen, K. *Chem. Mater.* **1997**, *9*, 1063.
10. Ikeda, S.; Hara, M.; Kondo, J.; Domen, K.; Takahashi, H.; Okubo, T.; Kakihana, M. *Chem. Mater.* **1998**, *10*, 72.
11. Gopalakrishnan, J.; Uma, S.; Bhat, V. *Chem. Mater.* **1993**, *5*, 132.
12. Hong, Y. -S.; Kim, S. -J.; Kim, S. -J.; Choy, J. -H. *J. Mater. Chem.* **2000**, *10*, 1209.
13. Byeon, S. -H.; Nam, H. -J. *Chem. Mater.* **2000**, *12*, 1771.
14. Dion, M.; Ganne, M.; Tournoux, M. *Mater. Res. Bull.* **1981**, *16*, 1429.
15. Gopalakrishnan, J.; Bhat, V. *Inorg. Chem.* **1987**, *26*, 4329.
16. Gopalakrishnan, J.; Bhat, V.; Raveau, B. *Mater. Res. Bull.* **1987**, *22*, 413.
17. Uma, S.; Raju, A. R.; Gopalakrishnan, J. *J. Mater. Chem.* **1993**, *3*, 709.
18. Wright, A. J.; Greaves, C. *J. Mater. Chem.* **1996**, *6*, 1823.
19. Bhuvanesh, N. S. P.; Crosnier-Lopez, M. P.; Duroy, H.; Fourquet, J. L. *J. Mater. Chem.* **1999**, *9*, 3093.